

J. BARAN,<sup>1</sup> N.A. DAVYDOVA,<sup>2</sup> M. DROZD,<sup>1</sup> E.A. PONEZHA,<sup>3</sup> V.YA. REZNICHENKO<sup>2</sup>

<sup>1</sup>Institute of Low Temperature and Structure Research, PAS  
(2, Okolna Str., Wroclaw, Poland)

<sup>2</sup>Institute of Physics, Nat. Acad. of Sci. of Ukraine  
(46, Prosp. Nauky, Kyiv 03680, Ukraine; e-mail: davydova@iop.kiev.ua)

<sup>3</sup>Bogolyubov Institute for Theoretical Physics, Nat. Acad. of Sci. of Ukraine  
(14b, Metrologichna Str., Kyiv 03680, Ukraine)

PACS 64.70.Pf, 64.70.Kt,  
64.60.Qb

## NATURE OF THE DYNAMIC CROSSOVER IN ORTHOTERPHENYL

*We have conducted the infrared spectroscopic study and differential scanning calorimetry measurements (DSC) on orthoterphenyl (OTP), aiming to explore the physical nature of the dynamic crossover at  $1.2T_g$  found in variety experiments on OTP. We have obtained that, at  $T \leq 1.2T_g$  ( $\sim 290$  K) in the supercooled liquid OTP, the crystal nuclei appear and are absent at higher temperatures. These results suggest that the origin of the dynamic crossover at  $1.2T_g$  is related to the formation of fluctuating nuclei in the supercooled liquid, as a temperature of  $1.2T_g$  is approached. Therefore, we would expect that the appearance of the nuclei would change the molecular dynamics from individual to cooperative.*

*Keywords:* differential scanning calorimetry, infrared spectroscopy, glass transition, nucleation, orthoterphenyl, supercooled liquids.

### 1. Introduction

A whole class of glass-forming liquids is characterized by the existence of the crossover temperature  $T_c \approx 1.2T_g$  within the mode coupling theory (MCT) [1–4]. The MCT describes the slowing down of the structural dynamics of a liquid in terms of the development of a non-linear coupling between density fluctuations that, in the idealized version, is responsible for the structural arrest at a critical temperature  $T_c$  above  $T_g$ . For the most glass-forming systems, including OTP, the supercooled phase below  $T_c$  has universal physical properties. In particular, the relaxation time  $\tau_\alpha$  ( $\tau_\alpha$  represents the time required for the liquid to return to the equilibrium state after a small perturbation) exhibits a temperature dependence stronger than the Arrhenius one [5–15].

It should be noted that, despite the fact that  $T_c$  is defined within the theory, some experiments demonstrate the model-independent evidence of  $T_c$ , at which some qualitative changes occur in the dynamics of glass-forming systems. Novikov and Sokolov [16] carefully studied the papers, where estimates of the crossover temperature  $T_c$  have been done for 26 various glass-forming systems, and demonstrated that

the structural relaxation time  $\tau_\alpha$  at  $T_c$  appears to be the same in most systems, including those that are covalent and hydrogen bonded, ionic, molecular, and polymeric.

The anomalous temperature dependence of the structural  $\alpha$ -relaxation, which is observed in various liquids and polymers irrespective of their detailed molecular properties, suggests a collective phenomenon involving the cooperative motion of a large number of molecules, the feature whose explanation has been the major focus of theoretical descriptions of the glass transition. Geometrical frustration has often been considered to play a key role in such phenomenon [17]. “Frustration” describes an incompatibility between the extension of the locally favored structures such as the icosahedral order in a liquid and the tiling of the whole space [17, 18]. The temperature at which the locally favored structures appear is associated with a temperature of a narrowly avoided phase transition  $T^*$  [17, 18]. In the works of Tanaka [19–22], it was proposed that there is a transition from the ordinary-liquid to the frustrated metastable-liquid state at  $T_m$ , which is characterized by the appearance of metastable high-density solid-like islands and the resulting appearance of the cooperative nature of the  $\alpha$ -relaxation. Blazhov *et al.* [23] considered the clusterization and nucleation processes

as the main physical mechanisms of the microinhomogeneous structure formation in highly viscous liquids. Computer simulations performed by Buchner and Heuer [24] showed that, in the supercooled regime, the dynamics is strongly influenced by the presence of deep valleys in the potential energy landscape, corresponding to long-lived metastable amorphous states. Fischer *et al.* [25] assumed the existence of local structures with energetically preferred configurations, which were termed “glassy clusters” or “nonperiodic solids”. These clusters have a limited lifetime given by the  $\alpha$ -relaxation time.

Although it has long been recognized that the dynamics in supercooled liquids below the crossover temperature is spatially heterogeneous, the physical origin of these locally favored structures, which start to appear at a crossover temperature when a liquid enters into the supercooling state upon cooling, has not been established even at a basic level.

Earlier, our studies [26, 27] of several different glass formers (2-biphenylmethanol, benzophenone and salol) have shown that, as the temperature  $T \sim 1.2T_g$  is approached, the crystal nuclei of the metastable phase start to appear in their supercooled liquid states. The precursors of nuclei originate in the local-density-fluctuation sites, which are already present in the quenching period of the supercooled liquid. Namely, they are responsible for the spatial and dynamic heterogeneities. These findings immediately raise the question whether the nucleation at  $T_c$  above  $T_g$ , which is responsible for the heterogeneity, is a universal physical property for supercooled liquids? To verify this suggestion, the organic glass former OTP was chosen, because OTP has received much attention among researches from both experimental and numerical simulation points of view [28–54]. The critical temperature  $T_c$  has been determined by depolarized-light-scattering and quasielastic neutron scattering [30, 31] and by optical Kerr effect experiments [32, 33] and was found to be  $T_c \cong 290$  K. Moreover, the decoupling of the rotational and translational diffusions in OTP has been found at  $T_c = 290$  K [28, 29]. OTP, which shows a strongly non-Arrhenius temperature dependence of the viscosity as  $T_g$  is approached, has been characterized as a “fragile” liquid [8, 9].

To clarify the physical nature of the dynamic crossover in OTP and to answer the question why the dynamics is spatially heterogeneous, we performed Fourier transmittance infrared (FT-IR) spectroscopy

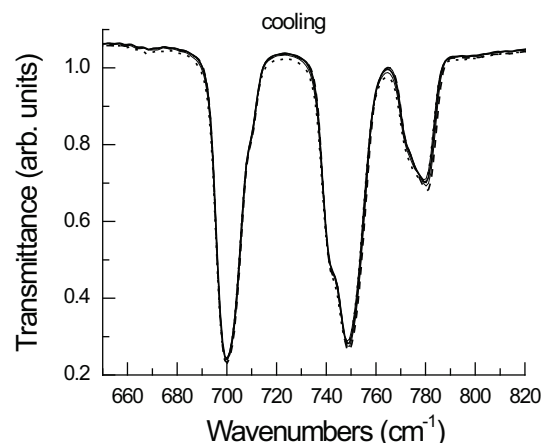


**Fig. 1.** Temperature-dependent FT-IR spectra for OTP recorded on cooling. Temperatures are (from bottom to top): 100, 180, 200, 240, and 300 K

and DSC measurements. This research will provide us with the explanation of the dynamic crossover in terms of the creation of fluctuating nuclei, when the supercooled liquid OTP approaches the crossover temperature  $T \sim 1.2T_g$  upon cooling from room temperature down to  $T_g$ .

## 2. Experimental

OTP (1,2-diphenylbenzene:  $C_{18}H_{14}$ ) purchased from Aldrich was purified by recrystallization from a methanol solution; as a result, a white prismatic crystals were obtained. OTP consists of small rigid molecular units which interact via weak non-directional van der Waals forces. Molecular structure of OTP is given in Fig. 1 of [52]. It is constituted by three phenyl rings, the two side rings being attached to the parent (i.e., central) ring by covalent bonds. Molecules such as OTP are the simplest system that can be supercooled and forms glass.

FT-IR measurements were done on a Fourier-transform infrared spectrometer (Bruker model IFS-88) at a resolution of  $2\text{ cm}^{-1}$ , and 32 scan were typically co-added for an individual spectrum. Data processing was performed with the OPUS software. For the IR-FT measurements, a sample of powder OTP was inserted in a cell with two CsI pellets at room temperature and then melted into a thin film. The thickness of such a cell was approximately a few micrometers. Such a sample with liquid OTP was then fixed in an Oxford Duplex closed-cycle cryostat,

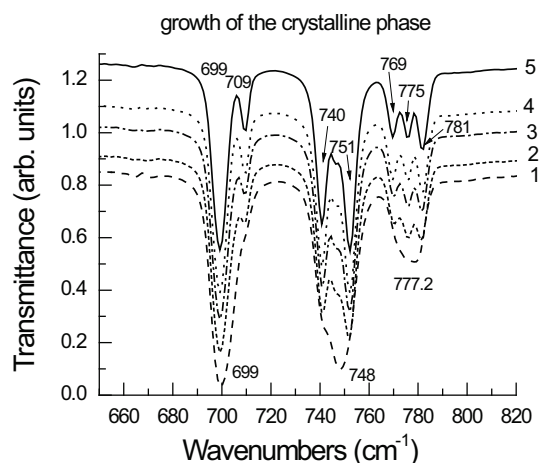


**Fig. 2.** FT-IR spectra variations for OTP recorded at  $T = 300$  K. Curve 1 is the spectrum recorded after the reheating of the glassy state; curves 2–5 were recorded in 5, 10, 15, and 20 min after recording curve 1

which allows working temperatures in the range 330–12 K with an accuracy of roughly 1 K.

DSC measurements were carried out in a Perkin-Elmer DSC-7 equipped with the CCA-7 low temperature accessory. A liquid nitrogen cooling system was used in order to reach the temperature as low as 104 K, and the measurements were carried out in the temperature range 104–343 K. A small amount of the sample ( $\sim 6.5$  mg) was enclosed in aluminum pans hermetically sealed with the use of a sample encapsulating press. Temperatures and enthalpies were calibrated using indium.

### 3. Results

#### 3.1. Infrared spectra

In this section, we will focus on the analysis of the FT-IR spectra of OTP. Infrared measurements were as follows: (1) a powder of crystalline OTP was melted in a cell with two CsI pellets; (2) the liquid sample was then cooled down to 100 K, and, during cooling, the FT-IR spectra were recorded (Fig. 1); (3) glassy OTP is then heated up to room temperature (300 K), and the FT-IR spectra were recorded for various waiting times (Fig. 2). We have studied the FT-IR spectra in the 400–4000  $\text{cm}^{-1}$  spectral range; however, as an example, we have chosen only the 650–820  $\text{cm}^{-1}$  spectral interval.

Figure 1 shows the fragments of the FT-IR transmittance spectra of the liquid OTP recorded on cool-

ing from room temperature (300 K) through the glass transition temperature down to 100 K. It is seen that the position and the shape of the bands in the IR spectrum during the transformation from the liquid to glass state are virtually unchanged. This means that, during cooling, the crystallization of the liquid state is avoided.

On the subsequent heating from the glass state through the glass transition to room temperature, the crystallization occurs. We analyzed the crystallization by continuously measuring the FT-IR spectra during isothermal aging performed at 300 K. The fragments of the FT-IR spectra are shown in Fig. 2. Dashed curve 1 shows the spectrum of the supercooled liquid phase recorded immediately after reaching the 300 K temperature. Next curves (2–5) were recorded in 5, 10, 15, and 20 min, respectively, after recording spectrum (1). It is seen that the crystallization process was completed within 20 min. The band at 772  $\text{cm}^{-1}$  in the process of crystallization transforms into three bands in the crystalline state spectrum: at 769, 775, and 781  $\text{cm}^{-1}$ . The band at 748  $\text{cm}^{-1}$  transforms into two bands in the crystalline state spectrum: 740 and 751  $\text{cm}^{-1}$ . The wide structureless band centered at 699  $\text{cm}^{-1}$  in the supercooled liquid state spectrum transforms into two bands at 699 and 709  $\text{cm}^{-1}$  in the crystalline state spectrum. The splitting appears more and more pronounced as the crystallization is completed (Fig. 2, solid curve 5). Not only in the spectral range presented in Fig. 2, but also in the whole region, the crystallization is manifested in the narrowing of bands and in the increase of their number. It should be noted that no changes in the IR spectra were observed, once the crystalline phase was obtained.

It is important that the supercooled liquid OTP is more stable in respect to the crystallization when we cool the liquid phase, than when we reheated the glassy phase through the glass transition region. This fact could be easily explained if we consider the shifts in the positions of two curves: crystal growth and crystal nucleation. The maximum rate of crystal nucleation is expected to appear at lower temperatures than that of the crystal growth. The process of nucleation begins in the supercooled liquid due to the fluctuation of the energy and is determined only by a thermodynamic factor. Nuclei of the crystalline phase are constantly appearing, growing, and disintegrating in the supercooled liquid. However, using

the IR spectroscopy method, we could observe only macroscopic processes, such as the crystallization or melting, whereas the nucleation being a relatively microscopic process is unobservable directly by this method. Thus, the IR spectra in the process of nucleation are practically unchanged (Fig. 1).

The growth process is controlled by the molecular diffusion process, and the transformation rate should be totally described as a thermal activation process. Thus, the growth of crystal nuclei via molecular collisions occurs at higher temperatures and lower viscosity, than the process of nucleation. To complete the crystallization, the system has to overcome an energy barrier that can be achieved by rising the temperature. Therefore, when we cool liquid OTP through the temperature region (high temperatures) at the maximum rate of crystal growth, the crystal nuclei are absent, so the crystallization is impossible. When we approach the temperature region (low temperatures) where the nucleation process starts, the viscosity is too high to allow nuclei to increase their radius. Thus, the nuclei, which emerge in the liquid sample during the quenching procedure, should be frozen into glass and comprise the glass structure.

### 3.2. Thermal behavior

Here, we will focus on the analysis of the DSC measurements in order to complement and to confirm the FT-IR results. Under heating, crystalline OTP melts at 332.14 K, which gives rise to an endothermic peak on a DSC scan (Fig. 3, dotted curve 1). The onset of the melting occurred at 330 K, and the melting enthalpy is  $78.29 \text{ Jg}^{-1}$  in agreement with the value reported by Steffen and co-workers [30]. After that, the sample was kept for 15 min at a temperature of 343 K, well above the melting temperature, in order to remove any nuclei that may be found. When this melted OTP is quenched at  $20 \text{ K min}^{-1}$  to 104 K, the crystallization is avoided (absence of an exothermic peak on the DSC scan) (Fig. 3, dashed curve 2). Only a heat flow jump can be clearly seen at 245.2 K (onset), which is the characteristic signature of the glass transition  $T_g$ . The heat capacity jump at the glass transition is  $-0.38 \text{ Jg}^{-1}\text{K}^{-1}$ . On the subsequent heating at  $20 \text{ K}\cdot\text{min}^{-1}$  to 343 K, the compound goes through the glass transition at  $T_g = 253 \text{ K}$  (onset) and the crystallization at 302 K (onset) and then melts at 332 K (endothermic peak on the DSC scan).

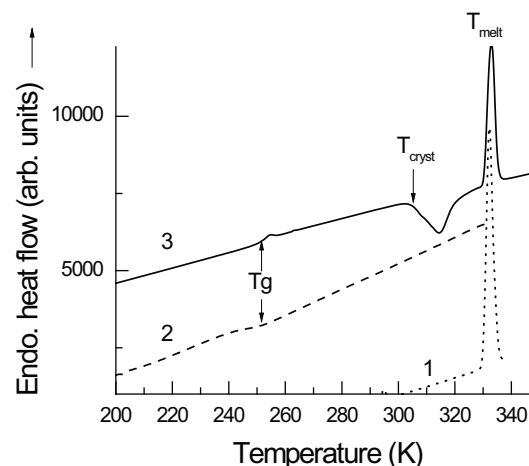


**Fig. 3.** DSC scans for OTP: (1) heating of the crystalline phase from 295 to 343 K; (2) cooling of the liquid state from 343 K to 104 K; (3) heating of the glassy state from 104 to 343 K. In the cooling-heating cycle, the scanning rate is  $20 \text{ K}\cdot\text{min}^{-1}$ . The sample mass is 6.5 mg

The heat capacity jump at the glass transition is  $0.58 \text{ Jg}^{-1}\text{K}^{-1}$  (Fig. 3, solid curve 3). It is seen that OTP in the supercooled liquid state is more stable in respect to the crystallization, when we cool liquid OTP, than when we reheat the glassy state.

As previously noted, the maximum rate of crystal nucleation is expected to appear at lower temperatures than that of the crystal growth. Our interest is in the determination of the temperature, at which the process of nucleation starts in OTP. For this purpose, we will use the DSC method. It should be noted that, by the DSC method, we could observe directly the macroscopic crystallization or melting, while the nucleation, being a relatively microscopic process, is unobservable directly by any method. However, the crystallization or melting peaks on DSC scans can be used as a detector to examine whether the nucleation process has or has not proceeded during heating, because the crystal growth presupposes the presence of crystal nuclei.

Figure 4 shows 8 DSC scans for OTP with a mass of 6.5 mg, all being obtained at a heating rate of  $20 \text{ K min}^{-1}$ . Each liquid sample for DSC measurements was previously quenched ( $200 \text{ K min}^{-1}$ ) from 343 K to the temperature  $T_n$  (precooling temperature) indicated in the figure and then measured on heating to examine if the crystallization (exothermic peak) or the melting (endothermic peak) appears on

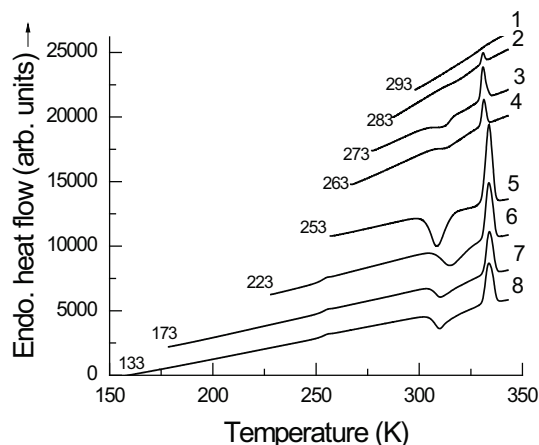


**Fig. 4.** DSC heating scans for OTP obtained at a heating rate of  $20 \text{ K}\cdot\text{min}^{-1}$ . Each sample was previously rapidly cooled at  $200 \text{ K}\cdot\text{min}^{-1}$  from  $343 \text{ K}$  to the temperature indicated in the figure and, after that, immediately reheated. The sample mass is  $6.5 \text{ mg}$

the DSC scans. Due to the fact that the crystallization begins with the formation of crystal nuclei, their formation can be judged from the appearance of corresponding peaks on a DSC scan. The DSC scans in Fig. 4 are vertically shifted for the sake of clarity. Scan 1 was obtained for the sample pre-cooled to  $293 \text{ K}$ . We have not seen any endothermic peak due to melting. The next scan 2 for the sample pre-cooled to  $283 \text{ K}$  shows a tiny endothermic peak due to the melting with a very small enthalpy ( $1.57 \text{ Jg}^{-1}$ ). The maximum intensity of the melting peak occurred at  $T_{\text{onset}} = 329.42 \text{ K}$  ( $T_m^{\text{max}} = 330.83 \text{ K}$ ). Consider that the melting peak presupposes the presence of crystal nuclei; we can conclude that the nucleation process in supercooled liquid OTP starts in the temperature range  $293\text{--}283 \text{ K}$ . Thus, in this temperature range, there exists a temperature  $T_n$  which separates two liquid states. Above  $T_n$ , we have to deal with a usual liquid, while the supercooled liquid below  $T_n$  is composed of nuclei coexisting with the supercooled liquid. A comparison of the temperature of the nuclei generation with a crossover temperature, at which the dynamics of supercooled liquid is drastically changed, that was determined in different experiments using neutron, light scattering, and optical Kerr effect methods [30–34], gives a good agreement. It follows directly from this observation that the origin of the crossover at  $1.2T_g$  is related to the

appearance of fluctuating crystalline nuclei in the supercooled liquid OTP at  $T \sim 1.2T_g$ .

For all samples pre-cooled below the glass transition temperature in the DSC heating scans, three essential features are seen (Fig. 4, curves 6–8). The first one corresponds to the glass transition at the temperature  $T_{g_{\text{onset}}} = 253 \text{ K}$ , and the second is an exothermic peak that corresponds to the crystallization and is observed in the temperature range  $302\text{--}313 \text{ K}$ . The third large endothermic melting peak at  $T = 329 \text{ K}$  indicates the melting of OTP. It is seen that the crystal growth occurs in the region  $302\text{--}313 \text{ K}$ , which is significantly separated by temperature from the crystal nucleation region  $293\text{--}283 \text{ K}$ . Thus, the presence of nuclei at low temperatures does not lead to the crystallization in the quenching period, which is consistent with the FT-IR results.

#### 4. Discussion

Judging from our experimental results, it is clear that the process of crystallization is observed only in the case where we heat OTP from the glassy state to room temperature, and it takes only a few minutes. However, a liquid sample may not be crystallized for a long time at room temperature. The fact that a liquid sample is not crystallized indicates that it does not contain nuclei, while the fluctuating nuclei emerge during the cooling procedure in the temperature range  $293\text{--}283 \text{ K}$  ( $1.2T_g\text{--}1.16T_g$ ). Such nuclei are constantly formed, grow, and disintegrate. So, they are responsible for the spatially heterogeneous dynamics in supercooled liquid OTP. Below  $T_g$ , these nuclei turn out to be incorporated in the glass structure. In the view of the fact that the crystal nuclei consist of an ordered arrangement of  $10\text{--}1000$  molecules, these ordered clusters in glassy OTP can be recognized as a measure of the heterogeneous nanostructure in glassy OTP. Thus, the glassy OTP is composed of solid regions (nuclei) (high density, low mobility), which are surrounded by weakly bounded regions, where the atomic motions are relatively fast (low density, high mobility). This view on the glass structure is consistent with some heterogeneous-structural models such as the Stillinger model [7], the island of mobility model by Johari and Goldstein [5], the entropy and density fluctuation model by Ediger [3], and the concept of cooperatively rearranging region and its correlation length by Donth [10].

Once a liquid OTP has been cooled to the temperature  $T_n$ , at which the nucleation starts, we would expect a change of the dynamics below this temperature from Arrhenius-like to non-Arrhenius, as was found, indeed, in a variety of experiments on OTP [35, 36, 40, 45, 49]. It follows directly from our results that the physical origin of the dynamic crossover is the appearance of fluctuating nuclei, as the temperature  $1.2T_g$  is approached.

## 5. Conclusion

We have studied the structural transformations of glass-forming OTP by the IR spectroscopy and DSC methods. The DSC method clearly provides evidence that, in the supercooled liquid OTP, fluctuating nuclei start to appear below  $T_n$ , which is close to the crossover temperature  $T_c \cong 1.2T_g$ , when the liquid enters into a supercooled state upon cooling. Above this temperature, we have to deal with a usual liquid; while, below  $1.2T_g$ , the supercooled liquid is composed of nuclei coexisting with the supercooled liquid. This means that, below  $T_n$ , the supercooled liquid is dynamically and spatially heterogeneous. In the supercooled liquid at high temperatures ( $> T_n$ ), crystalline nuclei are absent, so the crystallization is impossible even in the temperature interval 302–313 K at the maximum rate of crystal growth. The FT-IR spectroscopy method provides evidence that the crystalline nuclei expand into clusters of a macroscopic size, only when glassy OTP is heated. For the first time, we have obtained the FT-IR spectra of crystalline, supercooled liquid, and glassy states of OTP.

Based on our results, we can conclude that the nature of the dynamic crossover at  $1.2 T_g$  found in a variety of experiments on OTP is associated with the dynamics of creation and annihilation of nuclei. This is an interesting finding in light of our previous studies indicating that, at a crossover temperature  $\sim 1.2T_g$ , fluctuating nuclei also appear in the glass-formers: salol [27], benzophenone [27] and 2-biphenylmethanol [26]. Thus, the existence of nucleation near  $T_g$ , which determines the dynamic crossover, actually appears to be a universal feature of molecular glass formers.

1. E.W. Fischer, *Physica A* **201**, 183 (1993).
2. H. Sillescu, *J. Non-Cryst. Solids* **243**, 81 (1999).
3. M.D. Ediger, *J. Non-Cryst. Solids* **235-237**, 10 (1998).
4. R. Richert, *J. Phys.: Condens. Matter* **14**, R703 (2002).

5. G.P. Johari and M. Goldstein, *J. Chem. Phys.* **53**, 2372 (1970).
6. R.J. Greet and D. Turnbull, *J. Chem. Phys.* **46**, 1243 (1967).
7. F.H. Stiling, *J. Phys. Chem.* **89**, 6461 (1988).
8. C.A. Angel, K.L. Ngai, G.B. McKenna, P.F. McMillan, and S.W. Martin, *J. Appl. Phys.* **88**, 3113 (2000).
9. C.A. Angel, *J. Non-Cryst. Solids* **354**, 4703-4712 (2008).
10. E. Donth, *J. Non-Cryst. Solids* **53**, 325 (1982).
11. M.D. Ediger, C.A. Angel, and S.R. Nagel, *J. Chem. Phys.* **100**, 13200 (1996).
12. N.V. Surovtsev, S.V. Adichtchev, and V.K. Malinovsky, *Phys. Rev. E* **76**, 021502 (2007).
13. V.A. Popova, A.M. Pugachev, and N.V. Surovtsev, *Phys. Rev. E* **82**, 011503 (2010).
14. N.V. Surovtsev, *J. Phys.: Condens. Matter* **19**, 196101 (2007).
15. A.M. Brodin and E.A. Rossler, *J. Phys.: Condens. Matter* **18**, 8481 (2006).
16. V.N. Novikov and A.P. Sokolov, *Phys. Rev. E* **67**, 031507 (2003).
17. S.A. Kivelson, X. Zhao, D. Kivelson, T.M. Fisher, and C.M. Knober, *J. Chem. Phys.* **101**, 2391 (1994).
18. G. Tarjus, S.A. Kivelson, Z. Nussinov, and P. Viot, *J. Phys.: Condens. Matter* **17**, R1143, (2005).
19. S.A. Kivelson and G. Tarjus, *Nature Matter* **7**, 831 (2008).
20. H. Tanaka, *J. Phys.: Condens. Matter* **15**, L491 (2003).
21. H. Tanaka, *J. Non-Cryst. Solids* **351**, 3385 (2005).
22. H. Tanaka, *J. Non-Cryst. Solids* **351**, 678 (2005).
23. I.V. Blazhov, N.P. Malomuzh, and S.V. Lishchuk, *J. Chem. Phys.* **121**, 6435 (2004).
24. S. Buchner and A. Heuer, *Phys. Rev. Lett.* **84**, 2168 (2000).
25. E.W. Fischer, A. Bakai, A. Patkowski, W. Steffen, and L. Reinhardt, *J. Non-Cryst. Solids* **307-310**, 584 (2002).
26. J. Baran, N.A. Davydova, M. Drozd, and A. Pietraszko, *J. Phys.: Condens. Matter* **18**, 5695 (2006).
27. J. Baran, N.A. Davydova, and M. Drozd, *J. Phys.: Condens. Matter* **22**, 155108 (2010).
28. F. Fujara, B. Geil, H. Sillescu, and G. Fleischer, *Z. Phys. B* **88**, 195 (1992).
29. M.T. Cicerone and M.D. Ediger, *J. Chem. Phys.* **104**, 7210 (1996).
30. W. Steffen, A. Patkowski, H. Glaser, G. Meier, and E.W. Fischer, *Phys. Rev. E* **49**, 2992 (1994).
31. M. Kiebel, E. Bartsch, O. Debus, F. Fujara, W. Petry, and H. Sillescu, *Phys. Rev. B* **45**, 10301 (1992).
32. G. Hinze, D.D. Brace, S.D. Gottke, and M.D. Fayer, *Phys. Rev. Lett.* **84**, 2437 (2000).
33. S.D. Gottke, D.D. Brace, G. Hinze, and M.D. Fayer, *J. Phys. Chem. B* **105**, 238 (2001).
34. M.K. Mapes, S.F. Swallen, and M.D. Ediger, *J. Phys. Chem.* **110**, 507 (2006).
35. C.-Y. Wang and M.D. Ediger, *J. Phys. Chem. B* **103**, 4177 (1999).
36. M.T. Cicerone and M.D. Ediger, *J. Chem. Phys.* **103**, 56 (1995).

37. A. Barbieri, G. Gorini, and D. Leporini, *Phys. Rev. E* **69**, 061509 (2004).
38. L. Andreozzi, M. Faetti, and M. Giordano, *J. Non-Cryst. Solids* **352**, 3829 (2006).
39. R. Casalini and C.V. Roland, *Phys. Rev. Lett.* **92**, 245702 (2004).
40. A. Criado, F.J. Bermejo, A. Andres, and J.L. Martinez, *Mol. Phys.* **82**, 787 (1994).
41. L. Wu and S.R. Nagel, *Phys. Rev. B* **46**, 11198 (1992).
42. R. Bohmer, G. Diezemann, G. Hinze, and H. Sillescu, *J. Chem. Phys.* **108**, 890 (1998).
43. R. Bohmer, G. Hinze, G. Diezemann, B. Geil, and H. Sillescu, *Europhys. Lett.* **36**, 55 (1996).
44. C. Hansen, F. Stickel, T. Berger, R. Richert, and E. Fischer, *J. Chem. Phys.* **107**, 1086 (1997).
45. L.J. Lewis and G. Wahnstrom, *Phys. Rev. Lett.* **50**, 3865 (1994).
46. A. Biswas, *Appl. Spectrosc.* **47**, 458 (1993).
47. H.C. Semmelhack and P. Esquinazi, *Physica B* **254**, 14 (1998).
48. S. Mossa, R. Di Leonardo, G. Ruocco, and M. Sampoli, *Phys. Rev. E* **62**, 612 (2000).
49. S. Mossa, G. Ruocco, and M. Sampoli, *Phys. Rev. E* **64**, 021511 (2001).
50. A. Tolle, H. Zimmermann, F. Fujara, W. Petry, W. Schmidt, H. Schober, and J. Wuttke, *Eur. Phys. J. B* **16**, 73 (2000).
51. A. Tolle, J. Wuttke, H. Schober, O.G. Randl, and F. Fujara, *Eur. Phys. J. B* **5**, 231 (1998).
52. A. Tolle, *Rep. Prog. Phys.* **64**, 1473 (2001).
53. G.M. Brown and H.A. Levy, *Acta Crystallogr. Sect. B: Struct. Crystallogr. Cryst.* **35**, 785 (1979).
54. S. Aikawa, Y. Maruyama, Y. Ohashi, and Y. Sasada, *Acta Crystallogr. Sect. B: Struct. Crystallogr. Cryst.* **34**, 2901 (1978).

Received 23.09.2014

*Я. Баран, Н.О. Давидова,  
М. Дрозд, О.О. Понезжа, В.Я. Резніченко*

#### ПРИРОДА ДИНАМІЧНОГО КРОСОВЕРА В ОРТОТЕРФЕНІЛІ

#### Резюме

Ми використовували метод інфрачервоної спектроскопії й диференціально-скануючої калориметрії (ДСК) з метою встановлення фізичної природи динамічного кросовера при температурі  $1,2T_g$  в ортотерфенілі (ОТР), який був виявлен в багатьох експериментах на ОТР. Ми одержали, що при температурах  $T \leq 1,2T_g$  ( $\sim 290$  К) у переохолодженому рідкому ОТР утворюються кристалічні зародки, що відсутні при більш високих температурах. Ці результати свідчать, що природа динамічного кросовера при температурі  $1,2T_g$  пов'язана з утворенням флуктуюючих зародків у переохолодженої рідині при досягненні температури  $1,2T_g$ . Тому необхідно очікувати, що поява зародків приведе до зміни молекулярної динаміки від індивідуальної до кооперативної.